

RESEARCH ARTICLE

Open Access



Identification and characterization of in vivo, in vitro and reactive metabolites of vandetanib using LC–ESI–MS/MS

Mohamed W. Attwa^{1,2*}, Adnan A. Kadi¹, Hany W. Darwish^{1,2}, Sawsan M. Amer² and Nasser S. Al-shakliah¹

Abstract

Vandetanib (Caprelsa tablets, VNT) is an orally inhibitor of vascular endothelial growth factor receptor 2. The current research reports the characterization and identification of in vitro, in vivo and reactive intermediates of VNT. In vitro metabolites of VNT were performed by incubation with rat liver microsomes (RLMs). Extraction of vandetanib and its in vitro metabolites from the incubation mixtures were done by protein precipitation. In vivo metabolism was done by giving one oral dose of vandetanib (30.8 mg/kg) to Sprague Dawley rats in metabolic cages by using oral gavage. Urine was gathered then filtered at certain time intervals (0, 6, 12, 18, 24, 48, 72, 96 and 120 h) from vandetanib dosing. A similar volume of ACN was added to each collected urine sample. Both layers (organic and aqueous) were injected into liquid chromatography electro spray ionization tandem mass spectrometry (LC–ESI–MS/MS) to detect in vivo vandetanib metabolites. *N*-methyl piperidine ring of vandetanib is considered a cyclic tertiary amine that undergoes metabolism forming iminium intermediates that are very reactive toward nucleophilic macromolecules. Incubation of vandetanib with RLMs in the presence of 1.0 mM KCN was made to check reactive metabolites as it is usually responsible for noticeable idiosyncratic toxicities including phototoxicity and QT interval prolongation. Four in vivo phase I, one in vivo phase II metabolites, six in vitro phase I metabolites and four cyano conjugates of vandetanib were detected by LC–MS/MS. In vitro and in vivo phase I metabolic reactions were *N*-oxide formation, *N*-demethylation, α -carbonyl formation and α -hydroxylation. In vivo phase II metabolic reaction was direct conjugation of vandetanib with glucuronic acid. All metabolic reactions occurred in *N*-methyl piperidine of vandetanib which causes toxicity and instability of vandetanib.

Keywords: *N*-methyl piperidine, Vandetanib, In vivo metabolites, In vitro metabolites, Cyano conjugates

Introduction

Vandetanib (ZD6474) is an available orally inhibitor of vascular endothelial growth factor receptor 2 (VEGFR) [1]. VEGFR has gained great importance as pharmacologic targets as a Tyrosine kinase receptors [2]. Vandetanib, on 6 April 2011, was approved by the FDA for the treatment of patients suffered from symptomatic or progressive medullary thyroid cancer with unresectable, locally advanced, or metastatic disease. It was considered the first drug approved for this case. The trade name of

vandetanib was Caprelsa tablets (AstraZeneca Pharmaceuticals LP). Sudden death and QT prolongation of the are severe side effects for vandetanib [3].

Metabolism is detoxification process of xenobiotics and endogenous compounds by transforming into more hydrophilic compounds to allow excretion outside the body. Drug metabolism work is an essential step in the process of drug discovery, and is usually the factor that evaluate the degree of given drug success to take the approval and to reach the market [4]. Drug metabolism research is done through in vitro and in vivo techniques. In vivo metabolism was performed through the single dose administration of vandetanib to rat using oral gavage followed by gathering of urine samples, at specific time intervals, that contain the

*Correspondence: mzeidan@ksu.edu.sa; chemistzedan@yahoo.com

¹ Department of Pharmaceutical Chemistry, College of Pharmacy, King Saud University, P.O. Box 2457, Riyadh 11451, Kingdom of Saudi Arabia
Full list of author information is available at the end of the article



© The Author(s) 2018. This article is distributed under the terms of the Creative Commons Attribution 4.0 International License (<http://creativecommons.org/licenses/by/4.0/>), which permits unrestricted use, distribution, and reproduction in any medium, provided you give appropriate credit to the original author(s) and the source, provide a link to the Creative Commons license, and indicate if changes were made. The Creative Commons Public Domain Dedication waiver (<http://creativecommons.org/publicdomain/zero/1.0/>) applies to the data made available in this article, unless otherwise stated.

drugs and their possible metabolites. In vitro techniques include drugs incubation with various types of in vitro preparations (e.g. hepatocytes and liver microsomes) separated from rats then sample processing and analysis using chromatographic techniques.

Phase I metabolism either in vitro or in vivo of cyclic tertiary amines generates oxidative metabolites including: α -carbonyl formation, ring opening metabolites, *N*-oxygenation, ring hydroxylation and *N*-dealkylation. Metabolites are often less toxic than parent molecules, but occasionally undergo bioactivation forming unstable reactive intermediates that considered more toxic in comparison to parent molecules [5–7]. Reactive metabolites can covalently bind to proteins, which is considered the initiating step in the process of drug-induced organ toxicities [8, 9].

N-methyl piperidine ring is a part of vandetanib chemical structure that is considered a cyclic tertiary amine. Drugs that contain cyclic tertiary amine group are able to form iminium intermediates which are hard nucleophiles [10–12]. GSH or its derivatives are not the appropriate as capturing agent for hard nucleophiles while potassium cyanide (KCN) is the best agent for trapping these reactive intermediate including iminium ion [5] resulted in stable adducts formation which can be characterized, separated and detected using LC–MS/MS [13, 14].

Since bioactivation is often considered the central reason for observed side effects including phototoxicity and prolongation of QT interval [3, 15], we tested the reactive metabolites formation by incubation of vandetanib with 1.0 mM KCN. Upon literature review, *N*-demethyl vandetanib, vandetanib *N*-oxide and glucuronide conjugate were found in plasma, urine, and feces [1]. The full mechanism of bioactivation of vandetanib is not yet reported.

Chemicals and methods

Chemicals

All chemicals are mentioned in Table 1. Rat liver microsomes (RLMs) were prepared in house according to previously published protocol [16–20].

RLMs incubations

Vandetanib (20 μ mol/mL) was incubated at with RLMs (1.0 mg/mL), NADPH (1.0 mmol/mL) and K/Na phosphate buffer (50 mmol/mL, pH 7.4) containing $MgCl_2$ (3.3 mmol/mL). Incubation was done at thermostatted shaking water bath (37 °C) for 60 min before the reactions were quenched using two mL of ACN (ice-cold). The incubation mixtures were centrifuged at 14,000 rpm for 12 min then the supernatants were collected then subjected to dryness under a stream of N_2 . Samples residues were reconstituted in mobile

Table 1 List of chemicals and materials

Name ^a	Source
Dacomitinib	LC Laboratories (MA, USA)
Acetonitrile (ACN, HPLC-grade), ammonium formate (NH_4COOH), poly ethylene glycol 300 (PEG 300), dimethyl sulfoxide (DMSO), potassium cyanide (KCN) and formic acid ($HCOOH$)	Sigma-Aldrich (USA)
Tween 80	Eurostar Scientific Ltd. (Liverpool, UK)
Water (HPLC grade)	Milli-Q plus purification instrument (USA)
Sprague–Dawley rats ^b	The experimental animal care center at King Saud University (KSA)

^a All reference powders are of analytical grade and solvent are of HPLC grade

^b The University's Ethics Review Committee approved the animal experimental design

phase (95% solvent A and 5% solvent B). The same steps were repeated using a trapping agent (KCN at 1.0 mmol/mL) to capture reactive intermediates forming adducts.

In vivo metabolism of vandetanib

Six male Sprague–Dawley rats of average weight (340 g) and 4 weeks of age were brought from animal house of King Saud University (Riyadh, KSA). Each rat was housed in special metabolism cage that was placed in animal care facility in a 12-h light/dark cycle (7:00–19:00). Rats had free access to standard water and animal food. Rats were maintained in metabolism cages for 72 h before study starting. Vandetanib was formulated in special solution (5% Tween 80, 4% DMSO, 30% PEG 300, HPLC H_2O) to allow dispersion of vandetanib. Each rat received a calculated vandetanib depending on its weight.

The Recommended vandetanib dose is 300 mg per day until unacceptable toxicity or disease progression occurs. Average vandetanib dose for human is 5 mg/kg. Rat dose was calculated using these equations [21–23]:

$$\text{Rat (mg/kg)} = \text{Human (mg/kg)} * \text{Human Km/Rat Km}$$

$$\text{Rat (mg/kg)} = 5 * 37/6$$

$$\text{Rat (mg/kg)} = 185/6$$

$$\text{Rat (mg/kg)} = 30.8 \text{ (mg/kg)}$$

So the dose for rat was 30.8 mg/kg. Rats were given a single calculated dose of vandetanib. One rat was used as a control and was given solvent without vandetanib. Oral gavage was used for vandetanib dosing to rats. Urine samples were collected after draining into compartments fixed to metabolism cages before vandetanib dosing as

control sample and at specific time periods (6, 12, 18, 24, 48, 72, 96 and 120 h) following vandetanib dosing. Filtration of Urine samples was done using 0.45 μm syringe filters for discarding of particulate matters in the urine. A similar volume of ACN was added to each collected urine sample and then the resulted mixture was shaken by vortexing for 1 min. After storing the mixture at 4 °C overnight, two solvent layers (upper organic layer and lower aqueous layer) were formed. Both layers were evaporated until dryness under stream of N_2 and reconstituted respectively in 1 mL of mobile phase and transferred to HPLC Agilent vials for LC–MS/MS analysis. Control urine samples obtained from rats before drug dosing were done in the same way described for sample purification method. These samples were analyzed by LC–MS/MS to obtain control chromatograms.

Chromatographic conditions

The adjusted liquid and mass chromatographic conditions for the separation and identification of in vitro and in vivo vandetanib metabolites are described in details in Table 2.

Identification of in vitro metabolites, in vivo metabolites and cyano conjugates of vandetanib

Extracted ion chromatograms (EICs) for the vandetanib proposed metabolites were used to identify metabolites in the total ion chromatogram (TIC) of ether RLMs incubation extract or urine extract. CID of proposed metabolites molecular ion peaks (MIP) of was performed in the collision cell to get product ion (PI) mass spectra.

Structures of metabolites were done by reconstructing the product ions. In vivo vandetanib-related metabolites were concentrated in the organic layer while endogenous components of the urine and highly polar metabolites were located in the aqueous layer.

Results and discussion

Identification of in vitro phase 1 vandetanib metabolites

Six phase 1 metabolites were identified: one demethylated ($m/z - 14$) which was identified as VA461, two metabolites with one *N*-oxide or mono hydroxyl ($m/z + 16$) which were identified as VA491a and VA491b, one metabolite with oxidation of α -carbon and *N*-demethylation of *N*-piperidine which was identified as VA475 and two metabolites at m/z 489 which was identified as VA489a and VA489b (Table 3). Six metabolites were formed by incubation of vandetanib with RLMs through four metabolic reactions: *N*-demethylation, *N*-oxide formation, α -carbonyl formation, and α -hydroxylation (Table 3).

Identification of vandetanib and VA475 metabolite

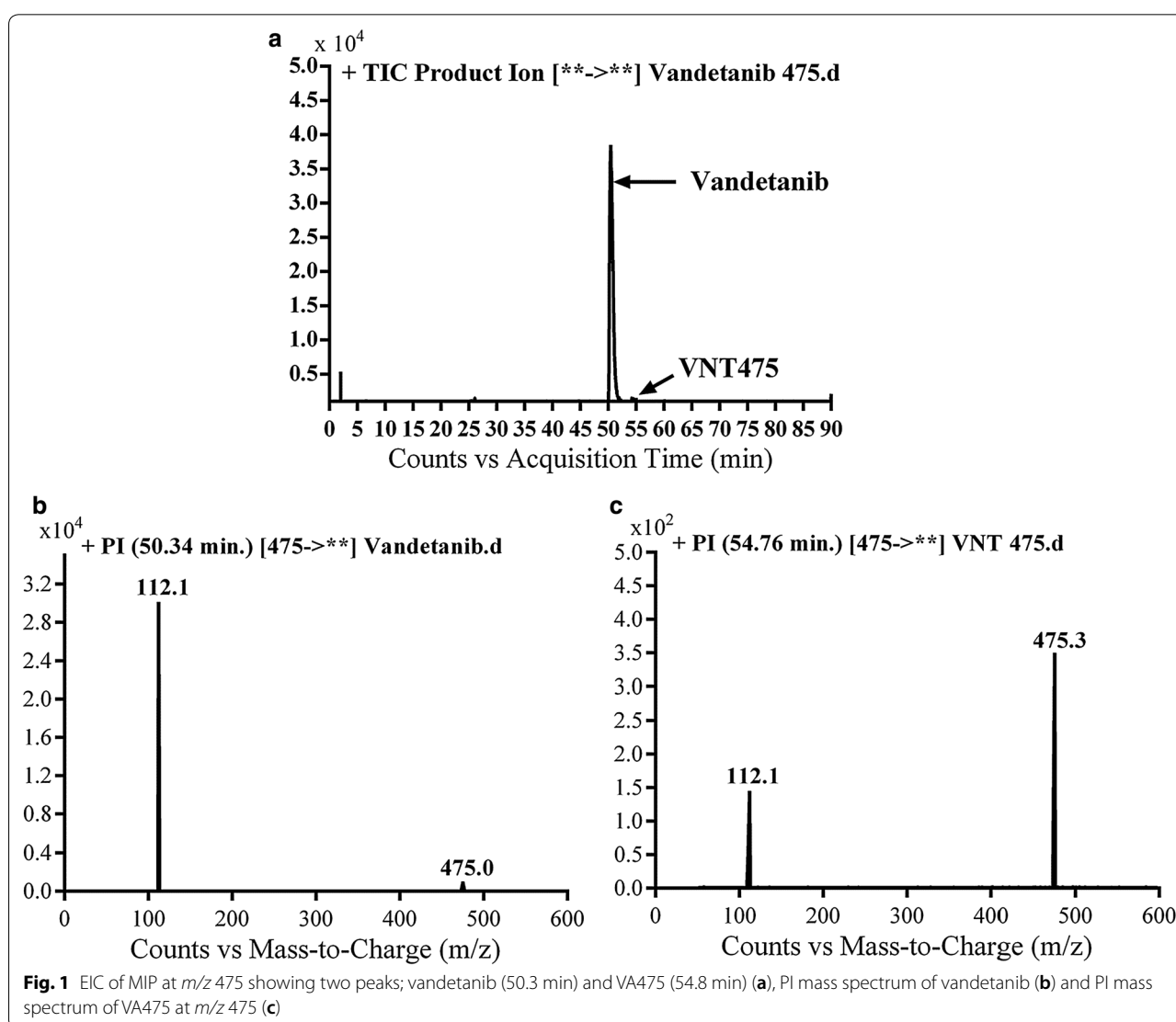
Vandetanib and VA475 metabolite MIPs were detected at m/z 475 in full MS scan mode at retention times (t_R) of 50.3 and 54.7 min, respectively (Fig. 1a). Upon CID of MIPs at m/z 475 gave different daughter ions (Fig. 1b). Collision induced dissociation (CID) of vandetanib inside collision cell of triple quadrupole at m/z 475 provided one daughter at m/z 112 (Fig. 1b). Daughter at m/z 112 represents methyl *N*-methyl piperidine moiety (Scheme 1).

Table 2 Optimized parameters of the established LC–MS/MS methodology

LC parameters		MS/MS parameters	
HPLC	Agilent 1200 (Agilent Technologies, CA, USA)	Mass spectrometer	Agilent 6410 QqQ (Agilent Technologies, CA, USA)
Mobile phase (gradient)	Aqueous phase: 10 mM Ammonium formate in H_2O (pH: 4.1 using Formic acid) Organic phase: ACN (0.1% Formic acid) Flow rate: 0.2 mL/min Elution time: 90 min	Ionization source	Positive electrospray ionization (ESI) Drying gas: N_2 gas Pressure (55 psi) Flow rate (12 L/min)
Agilent eclipse plus C_{18} Column	In vitro In vivo	ESI temperature: 350 °C Capillary voltage: 4000 V	
	Length (mm)	50	150
	Internal diameter (mm)	2.1	2.1
	Particle size (μm)	1.8	3.5
	Temperature:	22 \pm 2 °C	
Elution system	Time (min)	%B (ACN)	Collision gas
	0	5	N_2 (high purity)
	60	25	Modes
	80	70	Product ion (PI) and full mass scan and
	90	5	Mass Hunter software
	Post time 15	5	Vandetanib, in vivo, in vitro and reactive metabolites
			Mass conditions
			Fragmentor voltage (V)
			140
			Collision energy (eV)
			15

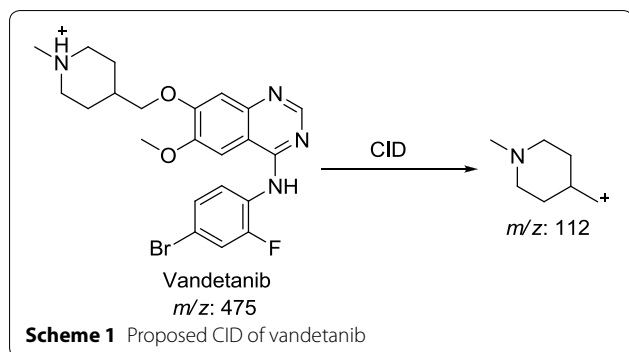
Table 3 Phase I metabolites of Vandetanib using MS scan and PI scan

	MS scan	Major daughter ions	t_R (min)	Metabolic pathway	Proposed conjugate composition	Previously detected (reference)
VNT	475	112	50.4		V+H	
VA461	461	364, 98	49.7	<i>N</i> -demethylation	V-CH ₂ +H	+ [1]
VA475	475	112, 110	54.7	<i>N</i> -demethylation and α oxidation	V-CH ₂ +O+H	
VA489a	489	126	66.8	α oxidation	V+O-2H+H	
VA489b	489	364	67.9	<i>N</i> -demethylation and 2 α oxidation	V-CH ₂ +2O+H	
VA491a	491	128, 111	57.1	α Hydroxylation	V+O+H	
VA491b	491	189, 128	50.4	<i>N</i> -oxidation	V+O+H	+ [1]



CID of VA475 MIP at m/z 475 gave daughters at m/z 112 and 110 in PI scan by QqQ MS (Fig. 1c). The fragment ion at m/z 112 proposed the removal of the methyl

group from the *N*-methyl piperidine and oxidation of α -carbon in the ring which matched with the other daughter ion at m/z of 110 (Scheme 2).



Identification of VA461 metabolite

VA461 metabolite of Vandetanib was detected at m/z 461 in full scan mode at t_R of 49.7 min (Fig. 2a). CID of MIP at m/z 461 generates fragment ion at m/z 98 (Fig. 2b). The daughter ion at m/z 98 supposed that the metabolic

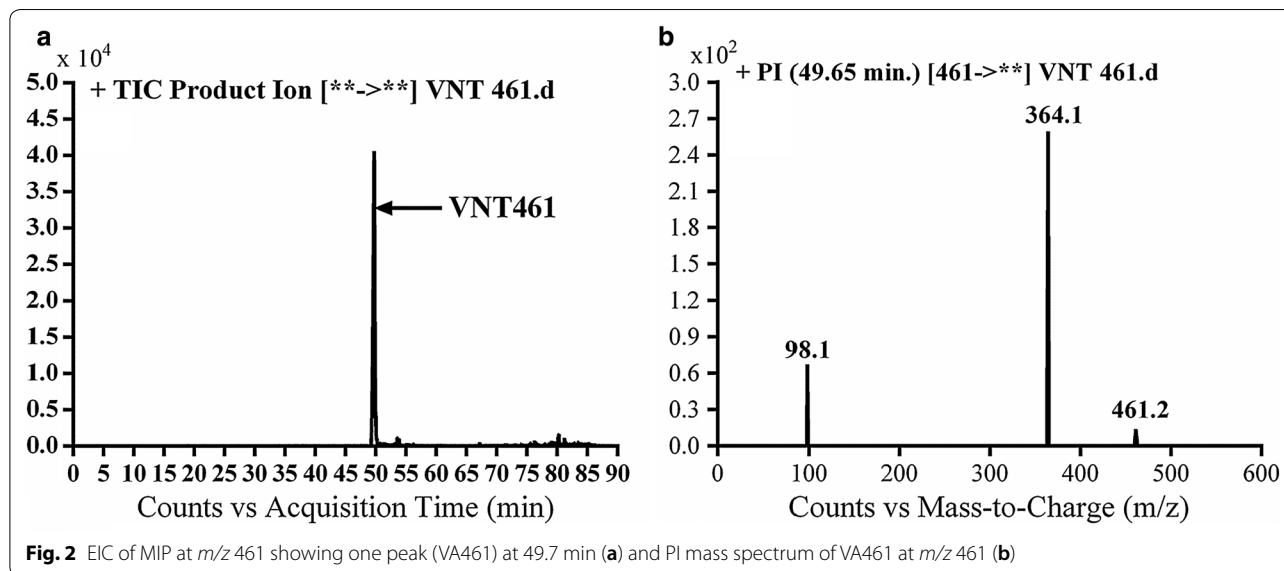
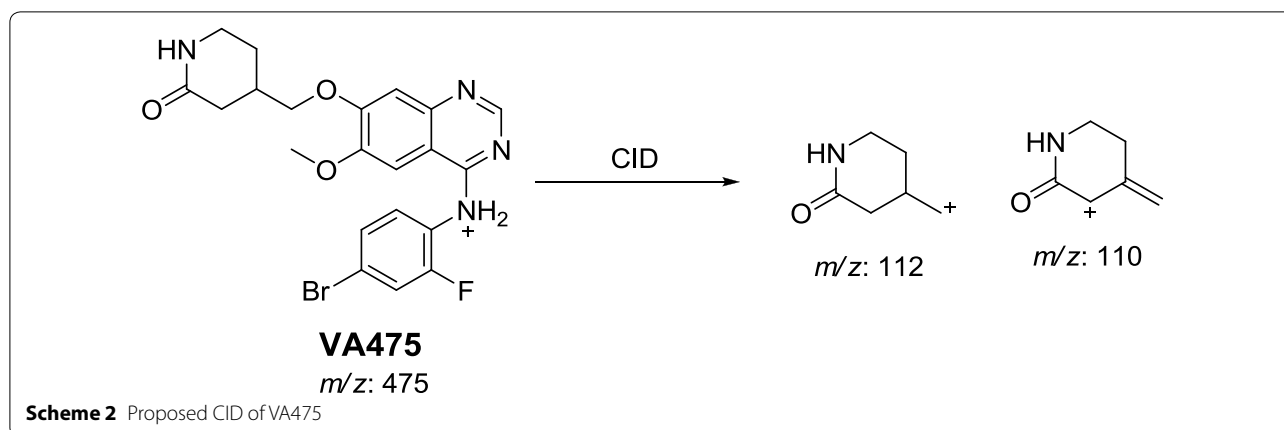
pathway is *N*-demethylation of the methyl group from the methyl piperidine ring, which matched with the other fragment ions at m/z 364. VA461 metabolite was the net product of removal of methyl group from *N*-methyl piperidine group in vandetanib (Scheme 3).

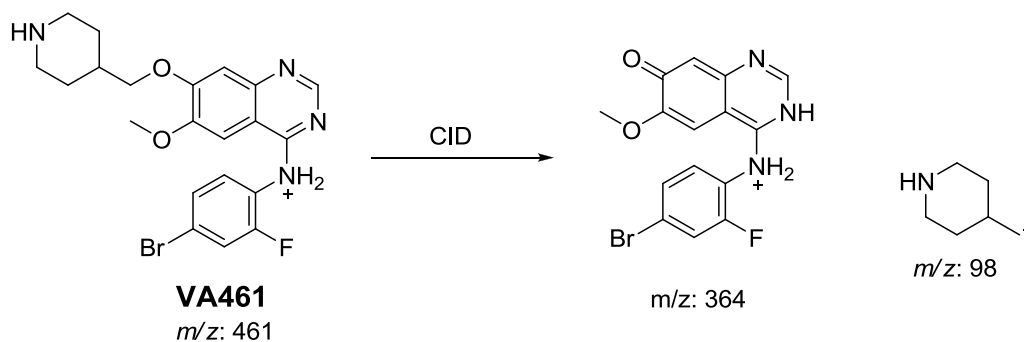
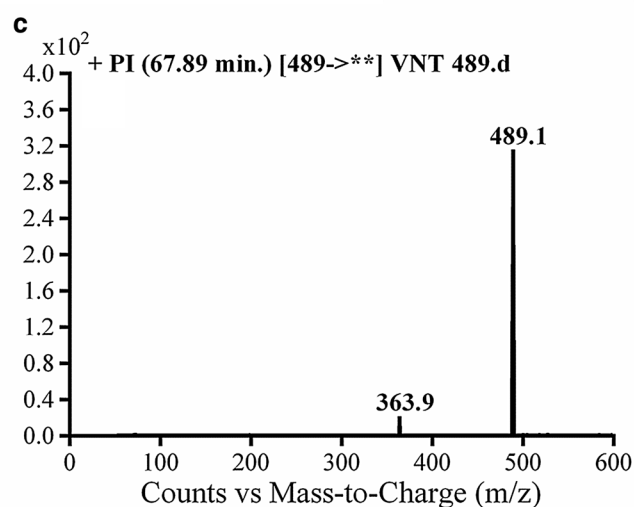
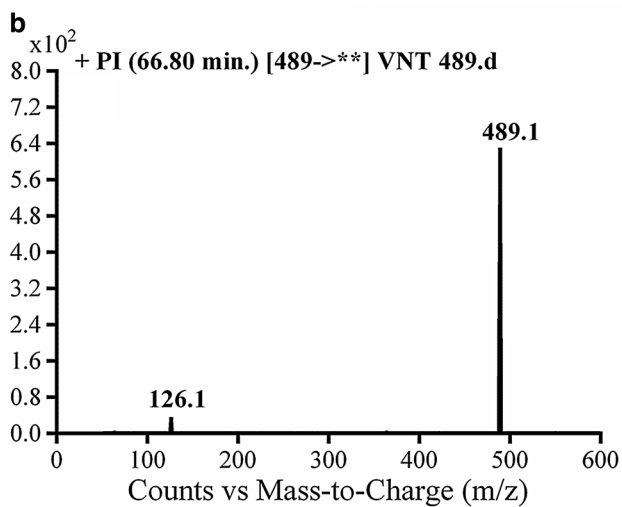
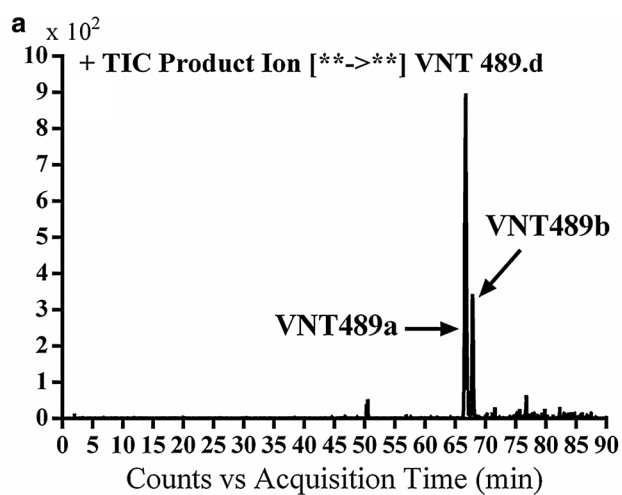
Identification of VA489 metabolite

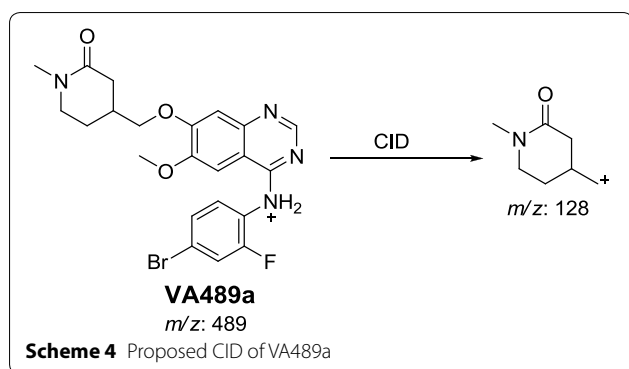
VA489a and VA489b metabolites of vandetanib were detected at m/z 489 in MS scan mode at t_R of 66.8 and 67.9 min, respectively (Fig. 3a). CID of MIPs at m/z 489 gave various daughter ions (Fig. 3b, c).

In case of VA489a, the fragment ion at m/z 126 supposed that the metabolic reactions were α -carbonyl formation of *N*-methyl piperidine group (Scheme 4).

In case of VA489a, the fragment ion at m/z 364 supposed that metabolic reactions were 2 α -carbonyl formation and *N*-demethylation at *N*-methyl piperidine ring (Scheme 5).



**Scheme 3** Proposed CID of VA461**Fig. 3** EIC of MIP at m/z 489 showing two peaks: VA489a (66.8 min) and VA489b (67.9 min) (a), PI mass spectra of VA489a (b) and VA489b at m/z 489 (c)



Identification of VA91a and VA491b metabolite

VA491a and VA491b metabolites of vandetanib were detected at m/z 491 in MS scan mode at t_R of 57.1 and 67.4 min, respectively (Fig. 4a). CID of MIPs at m/z 491 gave different daughter ions (Fig. 4b, c).

In the case of VA491a, the fragment ion at m/z 128 supposed that metabolic reaction was hydroxylation of α -carbon of *N*-methyl piperidine ring which matched with the daughter ion at m/z 111 (Scheme 6).

In case of VA491b, the fragment ion at m/z 128 proposed that *N*-oxide formation metabolic reaction occurred at *N*-methyl piperidine ring (Scheme 7).

Characterization of vandetanib reactive metabolites

Extracts of vandetanib in vitro incubations in the presence of 1.0 mM KCN with RLMs were injected into LC-QqQ. Identification of MIPs representing vandetanib cyanide conjugates was performed with mass scan and

PI scan for these peaks (Table 4). Four cyanide conjugates were identified, indicating that the *N*-methyl piperidine ring in vandetanib can become bioactivated and then captured by the nucleophile cyanide ion [19].

Identification of VB486 cyano conjugate of vandetanib

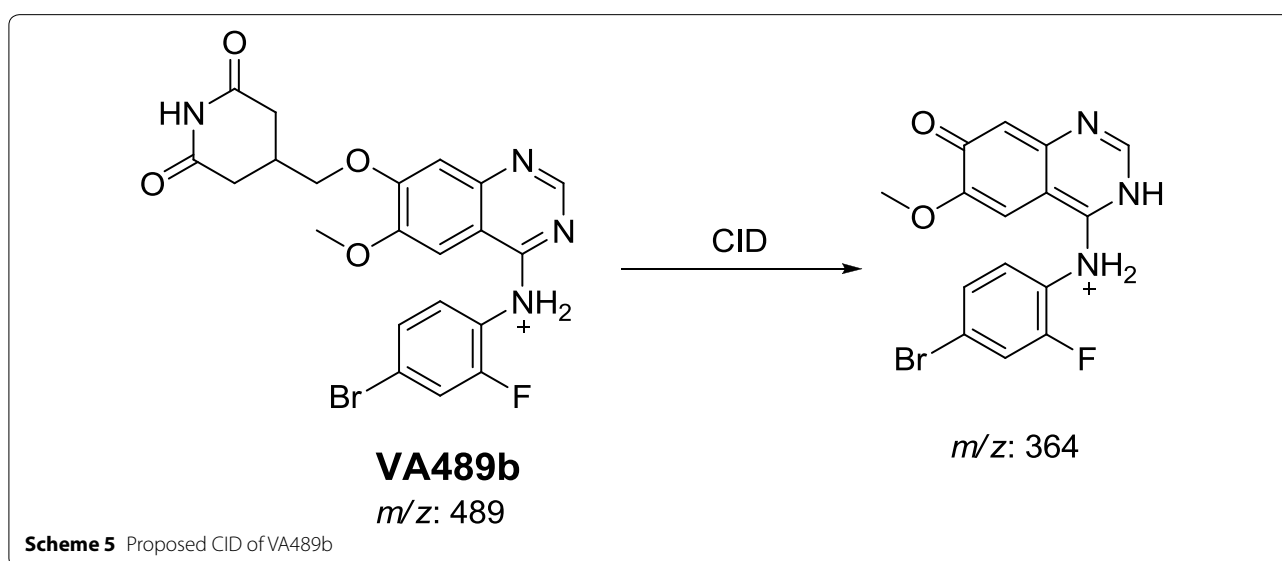
VB486 cyano conjugate was detected at m/z 486 in MS scan mode with t_R of 71.7 min. CID of MIP at m/z 486 generates fragment ions at m/z 363 and 389 (Fig. 5). The fragment ion at m/z 389 proposed cyano group addition to the bio activated α -carbon and *N*-demethylation of piperidine ring. The metabolic pathway in VB486 revealed to α -cyano *N*-demethyl vandetanib (Scheme 8).

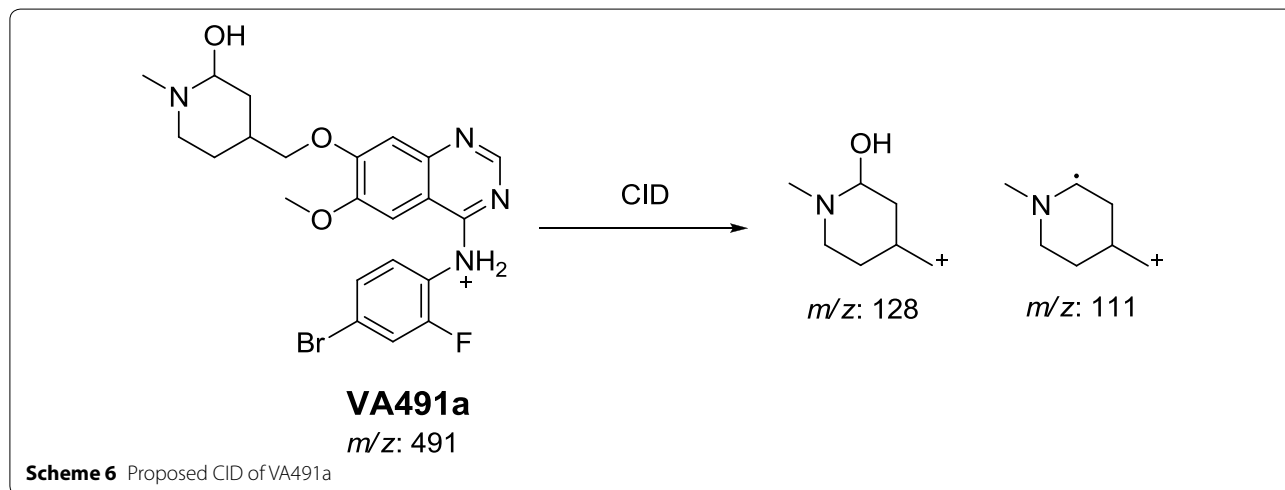
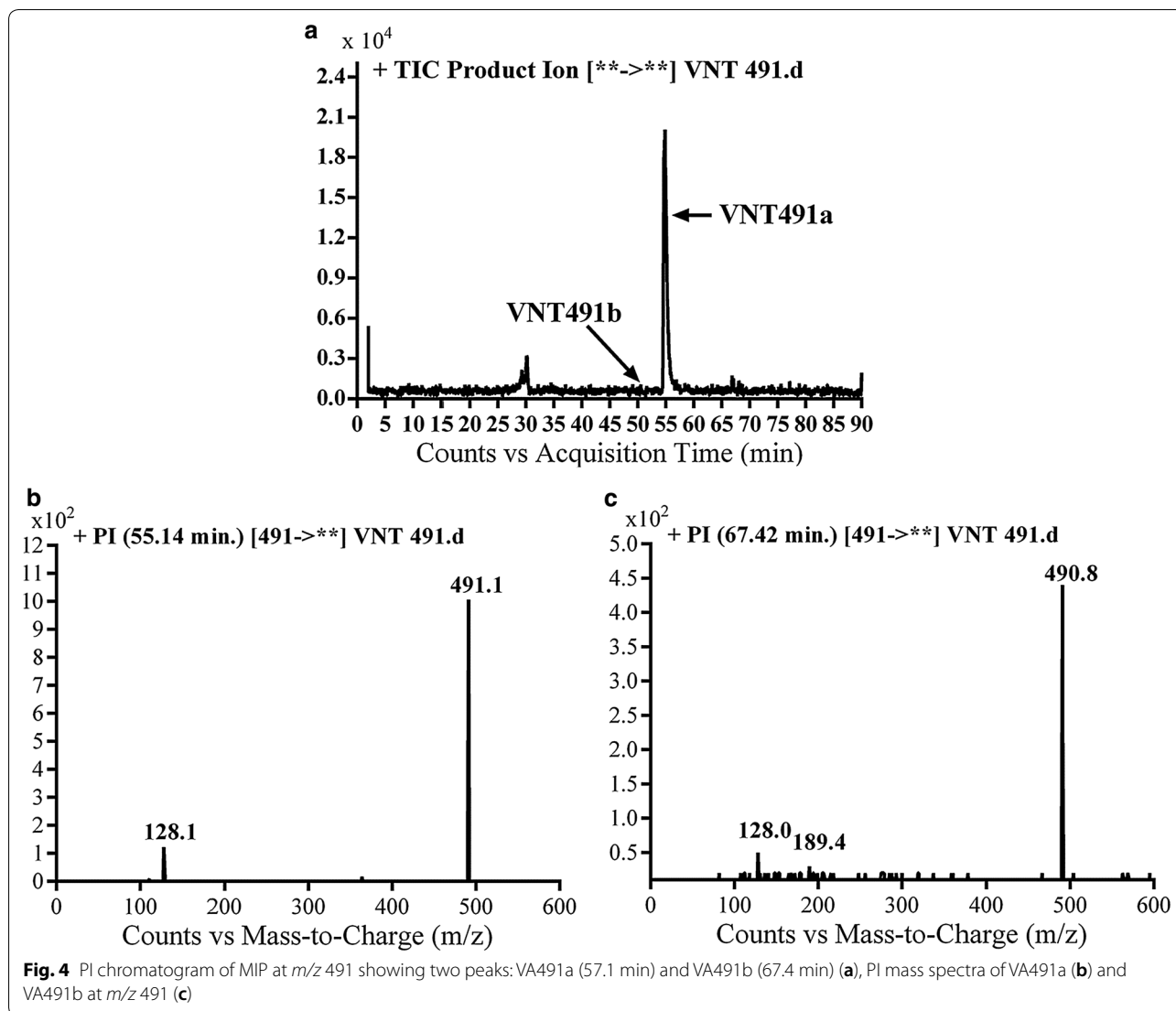
Identification of VB500a and VB500b cyano conjugates of vandetanib

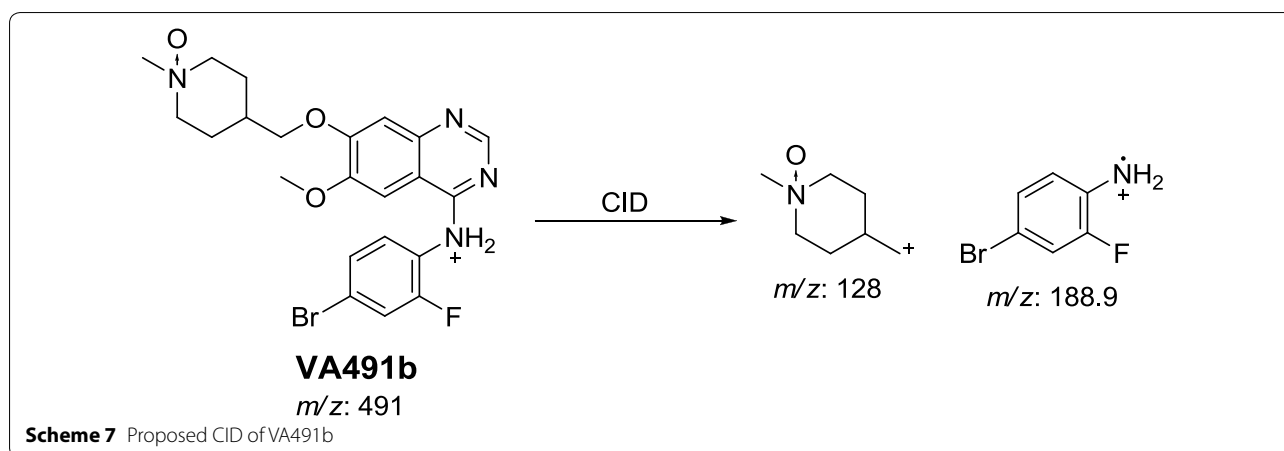
VB500a and VB500b cyano conjugates of vandetanib were detected at m/z 500 in MS scan mode with t_R of 68.4 and 76 min, respectively (Fig. 6a). CID of MIP at m/z 500 gave various fragment ions (Fig. 6b, c).

In case of VB500a, the fragment ion at m/z 137 proposed that cyano group addition occurred at activated α carbon of the methyl piperidine ring. The other fragment ion at m/z 473 represented the cyano group loss (Scheme 9). The metabolic pathway in VB500a revealed to α cyano vandetanib.

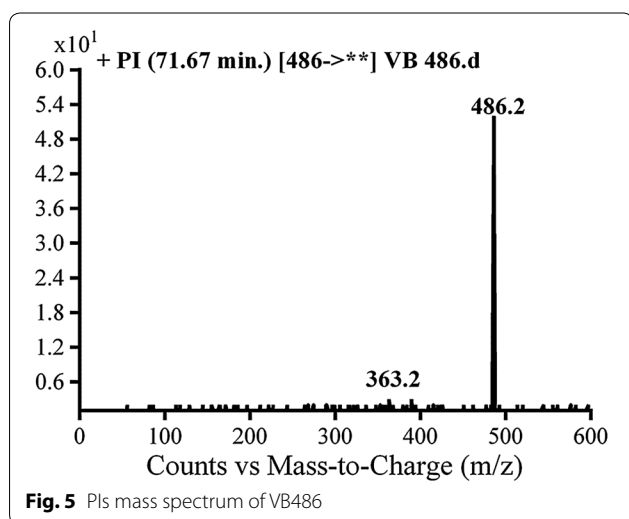
In case of VB500b, fragment ions at m/z 164 and m/z 457 proposed that α -carbonyl formation, *N*-demethylation and cyano group addition to the activated α carbon (Scheme 10). The metabolic reaction in VB500b revealed to α -cyano α -Keto *N*-demethyl vandetanib.





**Table 4** Vandetanib cyano conjugates

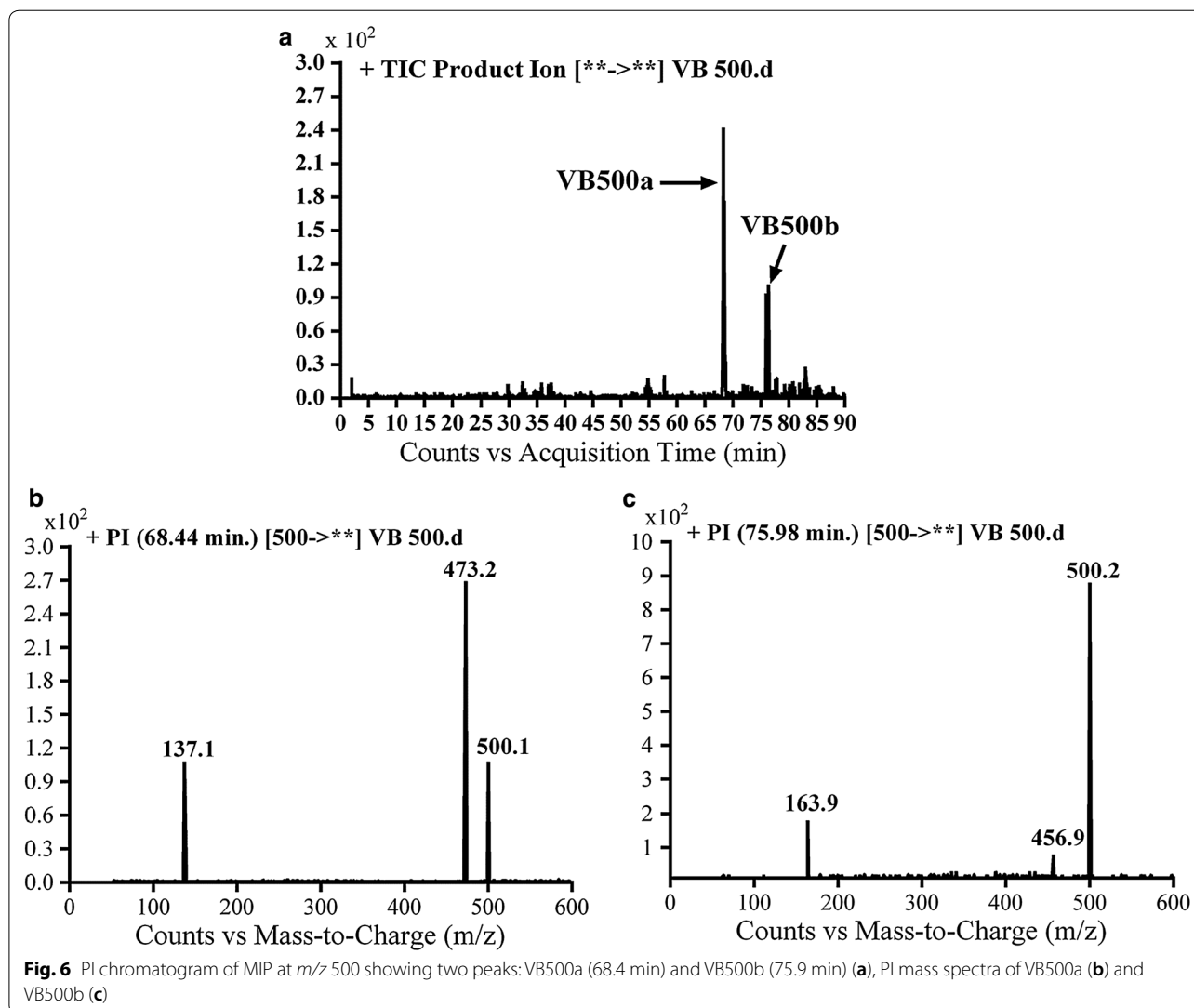
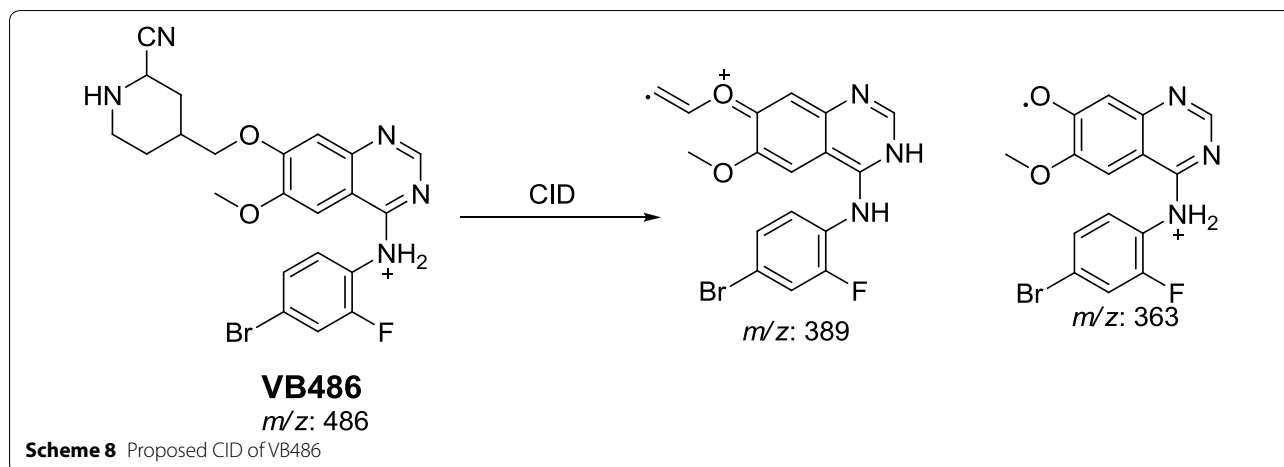
Code	MS scan	Major fragments	t_R (min)	Metabolic pathway	Postulated conjugate composition
VB486	486	389.4, 363.2	71.6	α Cyano addition and <i>N</i> -demethylation	V – CH ₃ + CN
VB500a	500a	373.2, 137.1	68.4	α Cyano addition	V + CN
VB500b	500b	456.9, 163.9	76	<i>N</i> -demethylation, α oxidation and α Cyano addition	V – CH ₃ + CN + O
VB502	502	484.3, 361.3, 287.4, 203.1	77.1	<i>N</i> -demethylation, α hydroxylation and α Cyano addition	V – CH ₃ + CN + OH

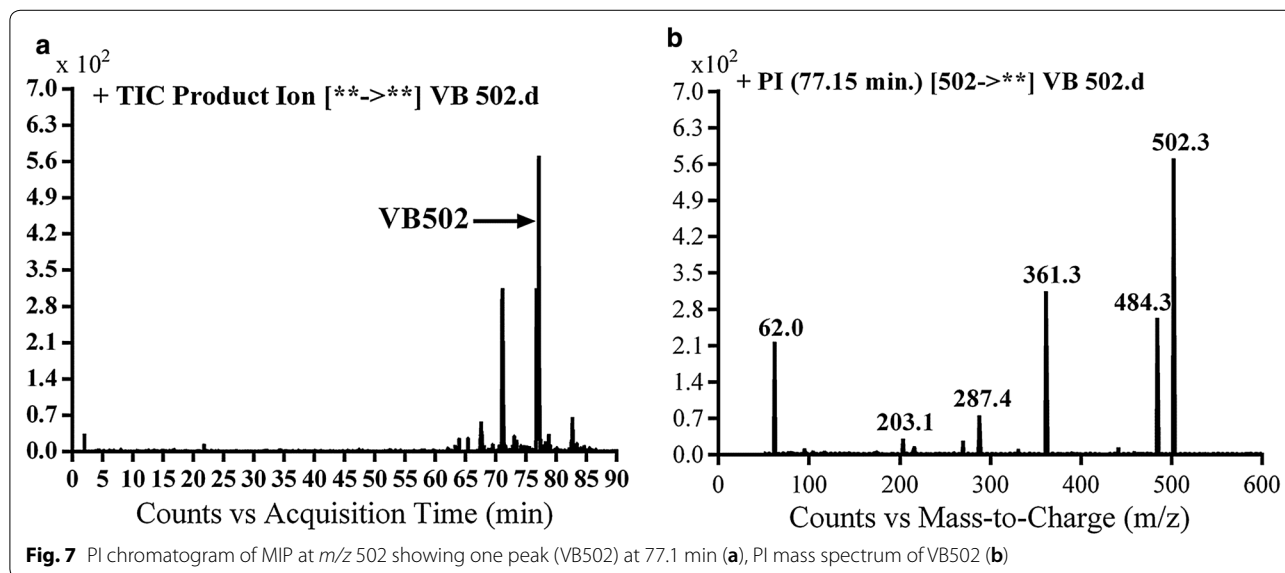
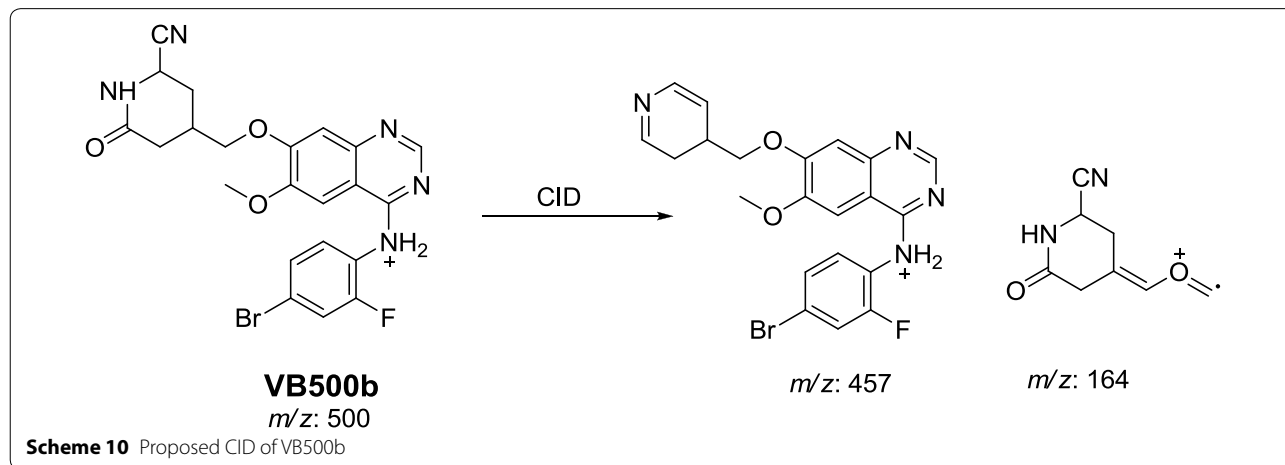
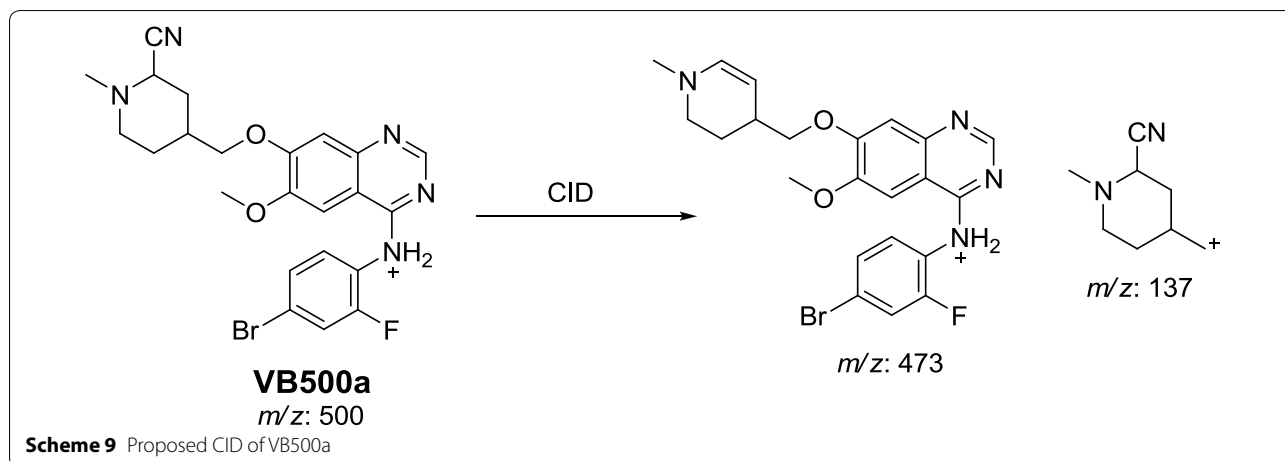
**Identification of VB502 cyano conjugate of vandetanib**

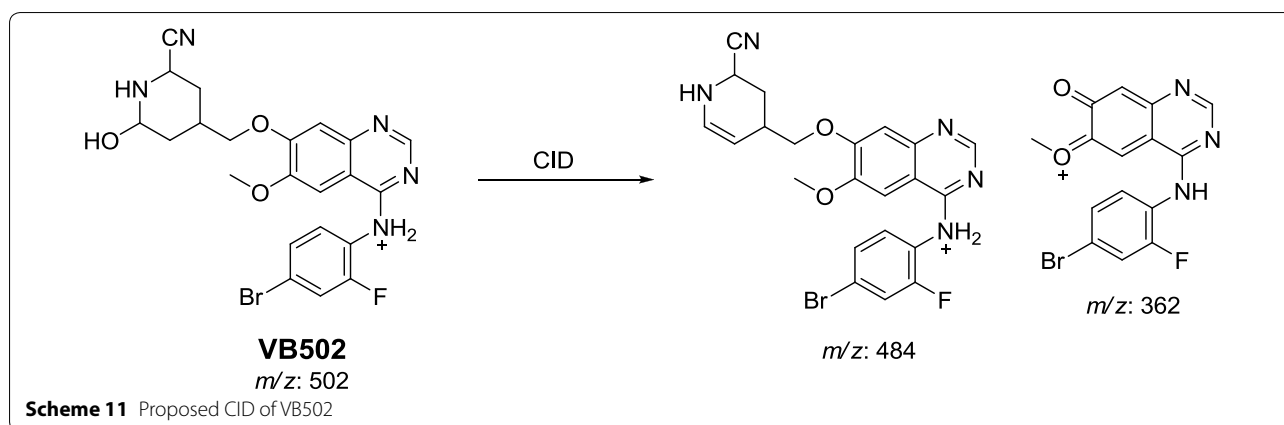
VB502 cyano adduct of vandetanib was detected at *m/z* 502 in MS scan mode at t_R of 77.1 min (Fig. 7a). CID of MIP at *m/z* 502 generates fragment ions at *m/z* 203, *m/z* 287, *m/z* 362 and *m/z* 484 (Fig. 7b). Daughter ion at *m/z* 362 supposed that all metabolic reactions happened in the piperidine group. Fragment ions at *m/z* 484 and *m/z* 362 proposed that hydroxylation of α carbon, *N*-demethylation of piperidine group and cyano group addition to the activated α -carbon piperidine ring (Scheme 11). The metabolic reaction in VB500b revealed to α -cyano α -hydroxyl vandetanib.

Bioactivation mechanism of vandetanib

Vandetanib contains cyclic tertiary amine group, *N*-methyl piperidine, that is able to form iminium intermediates which are reactive and can be captured







using KCN. The chemical structures of four cyanide conjugates of vandetanib were recognized and bio-activation reactions of the *N*-methyl piperidine ring were explained as shown in Scheme 12. The *N*-methyl piperidine ring in vandetanib underwent P450-catalyzed oxidation and/or hydroxylation and subsequent dehydration forming imine and imine-carbonyl intermediates (α,β -unsaturated) which was trapped by KCN to form stable conjugate that was characterized and detected in the tandem mass spectrometry detector [19, 20, 24, 25].

Identification of vandetanib in vivo metabolites

PI mass spectra comparison between control urine samples with urine extracts as well as PI comparison of vandetanib and proposed metabolites (Table 3) permitted the identification of four in vivo phase I and one phase II metabolites. Metabolic reactions for in vivo phase I metabolites were proposed to be *N*-oxide formation, *N*-demethylation and α -hydroxylation while for phase II metabolites were the result of *N*-conjugation of vandetanib with glucuronic acid. In vivo vandetanib phase I metabolites are previously mentioned in in vitro vandetanib phase I metabolism.

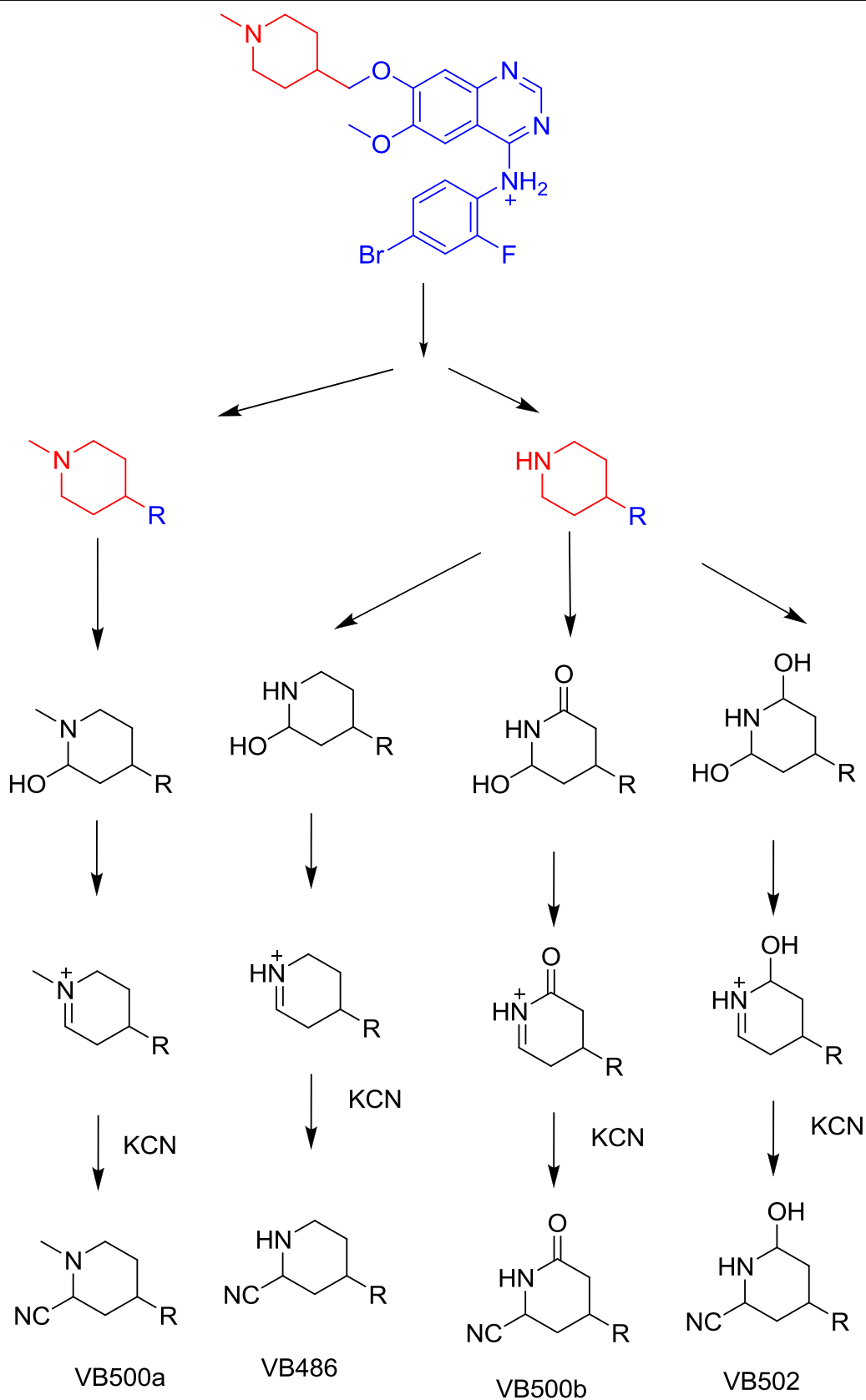
Excretion of vandetanib and its in vivo metabolites in rat urine

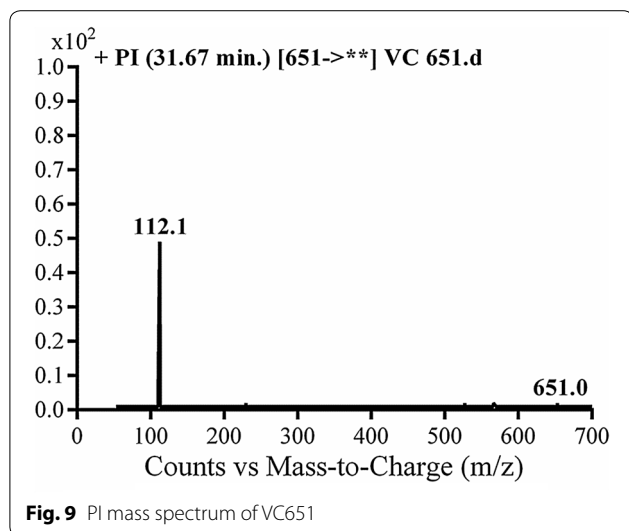
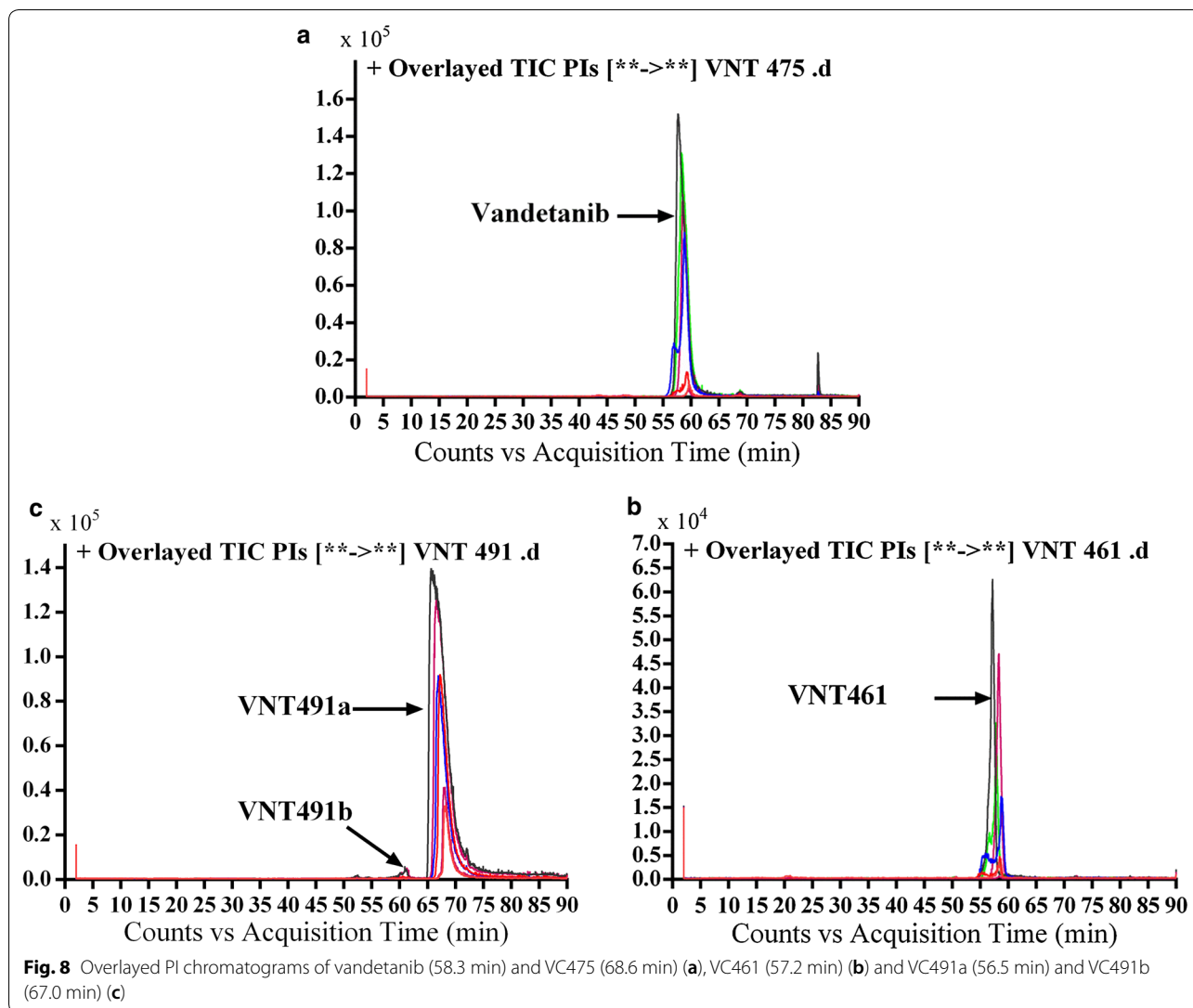
Part of vandetanib oral dose was excreted unchanged in rat urine. Vandetanib was detected at m/z 475 in

MS scan spectrum. Excretion of vandetanib and its in vivo phase I metabolites in urine were noticed after 6 h of dosing. Comparative concentration of vandetanib was high after 6 h and began to increase by time and reach maximum at 24 h and begin to decrease until almost disappeared after 120 h from dosing as indicated in the overlaid PI chromatograms for vandetanib and its in vivo phase I metabolites (Fig. 8). Comparison of vandetanib PIs with proposed peaks permitted the identification of metabolic changes in the found in vivo metabolites. All in vivo metabolites are similar to in vitro metabolites and the disappearance of α oxidation metabolic reaction in the in vivo metabolism.

Phase II vandetanib in vivo metabolites: glucuronic acid conjugates

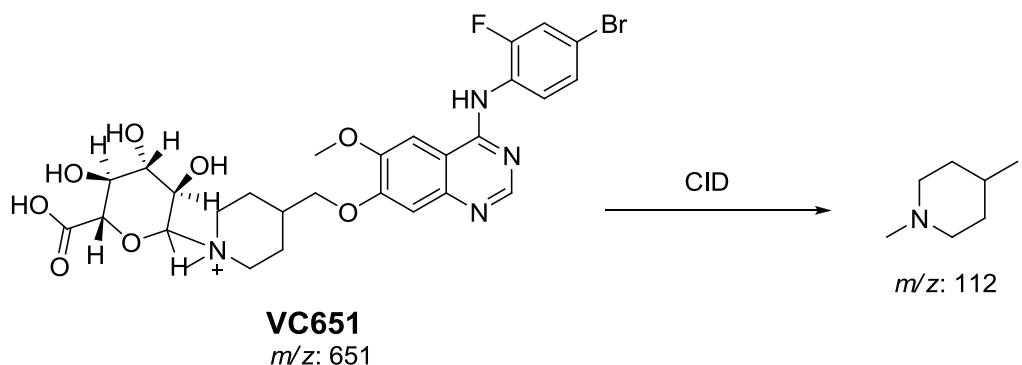
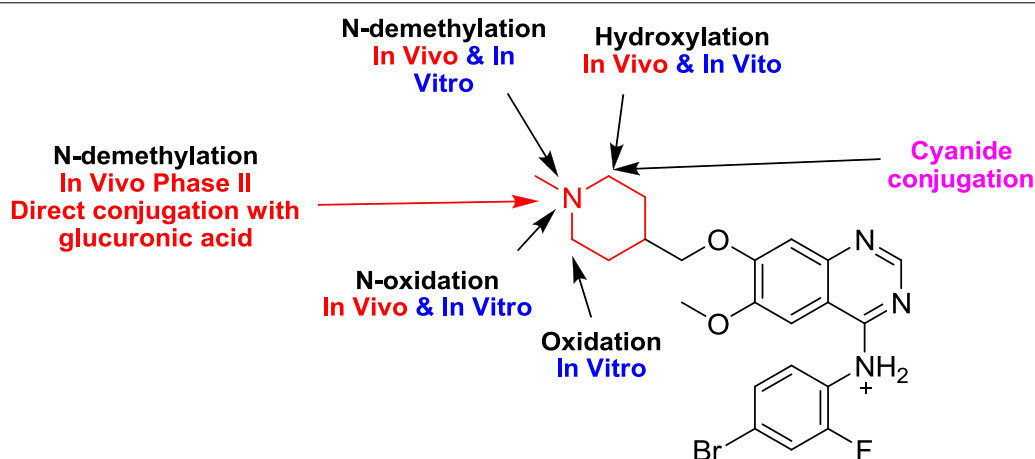
In vivo phase II metabolic reaction was direct conjugation of vandetanib with glucuronic acid. VC651 was located in the aqueous layer in a very small concentration in comparison to in vivo phase I metabolites. Excretion of in vivo phase II metabolites in urine was noticed after 24 h of rat dosing and vanished rapidly after 48 h of rat dosing. VC651 was detected at m/z 651 in MS scan spectrum of the aqueous layer urine extract. PI scan for VC651 at 31.7 min gave fragment ions at m/z 112 (Fig. 9). VC651 was proposed to be the result of direct conjugation of glucuronic acid with vandetanib (Scheme 13).

**Scheme 12** Bioactivation mechanism of piperidine ring of vandetanib



Conclusions

Four in vivo phase I, one in vivo phase II metabolites and six in vitro phase I were found for vandetanib. Phase I metabolic pathways for vandetanib were *N*-demethylation, *N*-oxide formation, α -carbonyl formation and α -hydroxylation. All phase I metabolic pathways happened in *N*-methyl piperidine of vandetanib (Fig. 10). Four cyano adducts were characterized. All metabolic and bioactivation reactions occurred in the *N*-methyl piperidine part which causes toxicity and instability of vandetanib (Additional file 1).

**Scheme 13** Proposed CID of VC651**Fig. 10** Proposed in vitro metabolites, in vivo metabolites and cyano conjugates of vandetanib

Additional file

Additional file 1: Figure S1. PI chromatograms of molecular ions at *m/z* 475 of organic extract of control urine sample taken before masitinib dosing showing no peaks at 58.3 min. and 68.6 min. **Figure S2.** PI chromatograms of molecular ions at *m/z* 461 of organic extract of control urine sample taken before vandetanib dosing showing no peak at 27.9 min. **Figure S3.** PI chromatograms of molecular ions at *m/z* 491 of organic extract of control urine sample taken before vandetanib dosing showing no peak at 56.5 and 67.0 min. **Figure S4.** Product ion chromatogram of molecular ion peak at *m/z* 475 showing two peaks: VC491a (56.5 min) and VC491b (67.0 min). **Figure S5.** PI mass spectrum of molecular ion peak (vandetanib) at *m/z* 475. **Figure S6.** PI mass spectrum of molecular ion peak (VC475) at *m/z* 475. **Figure S7.** Product ion chromatogram of molecular ion peak at *m/z* 461 showing one peak: VC461 (57.2 min). **Figure S8.** PI mass spectrum of molecular ion peak (VC461) at *m/z* 461. **Figure S9.** Product ion chromatogram of molecular ion peak at *m/z* 491 showing two peaks: VC491a (56.5 min) and VC491b (67.0 min). **Figure S10.** PI mass spectrum of molecular ion peak (VC491a) at *m/z* 491. **Figure S11.** PI mass spectrum of molecular ion peak (VC491b) at *m/z* 491.

Authors' contributions

MWA, AAK, HWD, and SMA established the experimental design. MWA run the research. MWA, HWD, SMA and AAK analyzed the data. HWD, NSA and MWA wrote the first draft of the manuscript. SMA, AAK and NSA contributed in editing the language of the manuscript. SMA, HWD and AAK follow up the

research steps. NSA made proofreading of the manuscript. All authors read and approved the final manuscript.

Author details

¹ Department of Pharmaceutical Chemistry, College of Pharmacy, King Saud University, P.O. Box 2457, Riyadh 11451, Kingdom of Saudi Arabia. ² Analytical Chemistry Department, Faculty of Pharmacy, Cairo University, Kasr El-Aini St, Cairo 11562, Egypt.

Acknowledgements

The authors would like to extend their sincere appreciation to the Deanship of Scientific Research at the King Saud University for funding this work through the Research Group Project No. RGP-322.

Competing interests

The authors declare that they have no competing interests.

Ethics approval and consent to participate

Animal Care Center Guidelines at College of Pharmacy of King Saud University were followed. Use Committee and Local Animal Care of King Saud University approved maintenance of rats.

Publisher's Note

Springer Nature remains neutral with regard to jurisdictional claims in published maps and institutional affiliations.

Received: 28 January 2018 Accepted: 19 September 2018
Published online: 24 September 2018

References

- Martin P, Oliver S, Kennedy SJ, Partridge E, Hutchison M, Clarke D et al (2012) Pharmacokinetics of vandetanib: three phase I studies in healthy subjects. *Clin Ther* 34(1):221–237
- Li F, Jiang S, Zu Y, Lee DY, Li Z (2014) A tyrosine kinase inhibitor-based high-affinity PET radiopharmaceutical targets vascular endothelial growth factor receptor. *J Nucl Med* 55(9):1525–1531
- Thornton K, Kim G, Maher VE, Chattopadhyay S, Tang S, Moon YJ et al (2012) Vandetanib for the treatment of symptomatic or progressive medullary thyroid cancer in patients with unresectable locally advanced or metastatic disease: U.S. Food and Drug Administration drug approval summary. *Clin Cancer Res* 18(14):3722–3730
- Kumar GN, Surapaneni S (2001) Role of drug metabolism in drug discovery and development. *Med Res Rev* 21(5):397–411
- Evans DC, Watt AP, Nicoll-Griffith DA, Baillie TA (2004) Drug-protein adducts: an industry perspective on minimizing the potential for drug bioactivation in drug discovery and development. *Chem Res Toxicol* 17(1):3–16
- Kalgutkar AS, Dalvie DK, O'Donnell JP, Taylor TJ, Sahakian DC (2002) On the diversity of oxidative bioactivation reactions on nitrogen-containing xenobiotics. *Curr Drug Metab* 3(4):379–424
- Boelsterli UA (2002) Xenobiotic acyl glucuronides and acyl CoA thioesters as protein-reactive metabolites with the potential to cause idiosyncratic drug reactions. *Curr Drug Metab* 3(4):439–450
- Knowles SR, Uetrecht J, Shear NH (2000) Idiosyncratic drug reactions: the reactive metabolite syndromes. *Lancet* 356(9241):1587–1591
- Ju C, Uetrecht J (2002) Mechanism of idiosyncratic drug reactions: reactive metabolites formation, protein binding and the regulation of the immune system. *Curr Drug Metab* 3(4):367–377
- Masic LP (2011) Role of cyclic tertiary amine bioactivation to reactive iminium species: structure toxicity relationship. *Curr Drug Metab* 12(1):35–50 (**Epub 2011/01/13**)
- Zhang Z, Chen Q, Li Y, Doss GA, Dean BJ, Ngui JS et al (2005) In vitro bioactivation of dihydrobenzoxathiin selective estrogen receptor modulators by cytochrome P450 3A4 in human liver microsomes: formation of reactive iminium and quinone type metabolites. *Chem Res Toxicol* 18(4):675–685
- Park BK, Boobis A, Clarke S, Goldring CE, Jones D, Kenna JG et al (2011) Managing the challenge of chemically reactive metabolites in drug development. *Nat Rev Drug Discov* 10(4):292–306
- Ma S, Zhu M (2009) Recent advances in applications of liquid chromatography–tandem mass spectrometry to the analysis of reactive drug metabolites. *Chem Biol Interact* 179(1):25–37
- Stepan AF, Walker DP, Bauman J, Price DA, Baillie TA, Kalgutkar AS et al (2011) Structural alert/reactive metabolite concept as applied in medicinal chemistry to mitigate the risk of idiosyncratic drug toxicity: a perspective based on the critical examination of trends in the top 200 drugs marketed in the United States. *Chem Res Toxicol* 24(9):1345–1410
- Salvador A, Vedaldi D, Brun P, Dall'Acqua S (2014) Vandetanib-induced phototoxicity in human keratinocytes NCTC-2544. *Toxicol In Vitro* 28(5):803–811
- von Jagow R, Kampffmeyer H, Kiese M (1965) The preparation of microsomes. *Naunyn-Schmiedeberg's Archiv für experimentelle Pathologie und Pharmakologie* 251(1):73–87
- von Jagow R, Kampffmeyer H, Kiese M (1965) The preparation of microsomes. *Naunyn-Schmiedeberg's Archiv für experimentelle Pathologie und Pharmakologie*. 251(1):73–87 (**Epub 1965/06/01**)
- Kadi AA, Attwa M, Darwish HW (2018) LC–ESI-MS/MS reveals the formation of reactive intermediates in brigatinib metabolism: elucidation of bioactivation pathways. *RSC Adv* 8(3):1182–1190
- Amer SM, Kadi AA, Darwish HW, Attwa MW (2017) Identification and characterization of in vitro phase I and reactive metabolites of masitinib using a LC–MS/MS method: bioactivation pathway elucidation. *RSC Adv* 7(8):4479–4491
- Kadi AA, Darwish HW, Attwa MW, Amer SM (2016) Detection and characterization of ponatinib reactive metabolites by liquid chromatography tandem mass spectrometry and elucidation of bioactivation pathways. *RSC Adv* 6(76):72575–72585
- Shin J-W, Seol I-C, Son C-G (2010) Interpretation of animal dose and human equivalent dose for drug development. *J Korean Med* 31(3):1–7
- Nair AB, Jacob S (2016) A simple practice guide for dose conversion between animals and human. *J Basic Clin Pharm* 7(2):27–31
- Reagan-Shaw S, Nihal M, Ahmad N (2008) Dose translation from animal to human studies revisited. *FASEB J* 22(3):659–661 (**Epub 2007/10/19**)
- Argoti D, Liang L, Conteh A, Chen L, Bershas D, Yu C-P et al (2005) Cyanide trapping of iminium ion reactive intermediates followed by detection and structure identification using liquid chromatography–tandem mass spectrometry (LC–MS/MS). *Chem Res Toxicol* 18(10):1537–1544
- Kadi AA, Amer SM, Darwish HW, Attwa MW (2017) LC–MS/MS reveals the formation of aldehydes and iminium reactive intermediates in foretinib metabolism: phase I metabolic profiling. *RSC Adv* 7(58):36279–36287

Ready to submit your research? Choose BMC and benefit from:

- fast, convenient online submission
- thorough peer review by experienced researchers in your field
- rapid publication on acceptance
- support for research data, including large and complex data types
- gold Open Access which fosters wider collaboration and increased citations
- maximum visibility for your research: over 100M website views per year

At BMC, research is always in progress.

Learn more biomedcentral.com/submissions



Terms and Conditions

Springer Nature journal content, brought to you courtesy of Springer Nature Customer Service Center GmbH (“Springer Nature”).

Springer Nature supports a reasonable amount of sharing of research papers by authors, subscribers and authorised users (“Users”), for small-scale personal, non-commercial use provided that all copyright, trade and service marks and other proprietary notices are maintained. By accessing, sharing, receiving or otherwise using the Springer Nature journal content you agree to these terms of use (“Terms”). For these purposes, Springer Nature considers academic use (by researchers and students) to be non-commercial.

These Terms are supplementary and will apply in addition to any applicable website terms and conditions, a relevant site licence or a personal subscription. These Terms will prevail over any conflict or ambiguity with regards to the relevant terms, a site licence or a personal subscription (to the extent of the conflict or ambiguity only). For Creative Commons-licensed articles, the terms of the Creative Commons license used will apply.

We collect and use personal data to provide access to the Springer Nature journal content. We may also use these personal data internally within ResearchGate and Springer Nature and as agreed share it, in an anonymised way, for purposes of tracking, analysis and reporting. We will not otherwise disclose your personal data outside the ResearchGate or the Springer Nature group of companies unless we have your permission as detailed in the Privacy Policy.

While Users may use the Springer Nature journal content for small scale, personal non-commercial use, it is important to note that Users may not:

1. use such content for the purpose of providing other users with access on a regular or large scale basis or as a means to circumvent access control;
2. use such content where to do so would be considered a criminal or statutory offence in any jurisdiction, or gives rise to civil liability, or is otherwise unlawful;
3. falsely or misleadingly imply or suggest endorsement, approval, sponsorship, or association unless explicitly agreed to by Springer Nature in writing;
4. use bots or other automated methods to access the content or redirect messages
5. override any security feature or exclusionary protocol; or
6. share the content in order to create substitute for Springer Nature products or services or a systematic database of Springer Nature journal content.

In line with the restriction against commercial use, Springer Nature does not permit the creation of a product or service that creates revenue, royalties, rent or income from our content or its inclusion as part of a paid for service or for other commercial gain. Springer Nature journal content cannot be used for inter-library loans and librarians may not upload Springer Nature journal content on a large scale into their, or any other, institutional repository.

These terms of use are reviewed regularly and may be amended at any time. Springer Nature is not obligated to publish any information or content on this website and may remove it or features or functionality at our sole discretion, at any time with or without notice. Springer Nature may revoke this licence to you at any time and remove access to any copies of the Springer Nature journal content which have been saved.

To the fullest extent permitted by law, Springer Nature makes no warranties, representations or guarantees to Users, either express or implied with respect to the Springer nature journal content and all parties disclaim and waive any implied warranties or warranties imposed by law, including merchantability or fitness for any particular purpose.

Please note that these rights do not automatically extend to content, data or other material published by Springer Nature that may be licensed from third parties.

If you would like to use or distribute our Springer Nature journal content to a wider audience or on a regular basis or in any other manner not expressly permitted by these Terms, please contact Springer Nature at

onlineservice@springernature.com